ACOUSTIC HALOS IN THE SOLAR ATMOSPHERE

आर्यभट्ट प्रेक्षण विज्ञान शोध संस्थान
Aryabhatta Research Institute of Observational Sciences

IISER
THIRUVANANTHAPURAM

Under the Guidance of

Dr. S. Krishna Prasad

By

Karthik SB

MSC22411

Master of Science

Department of Physics

INDIAN INSTITUTE OF SCIENCE EDUCATION AND RESEARCH

THIRUVANANTHAPURAM - 695 551, INDIA

August 2023

Declaration

I, “Karthik SB” (Roll No. MSC22411), hereby declare that, this report entitled “ACOUSTIC HALOS IN THE SOLAR ATMOSPHERE” submitted to Aryabhatta Research Institute of Observational Sciences towards the requirement of Visiting Student Program, is an original work carried out by me under the supervision of Dr. S. Krishna Prasad. I have sincerely tried to uphold academic ethics and honesty. Whenever a piece of external information or statement or result is used then, that has been duly acknowledged and cited.

Dated: 04/08/2023

Acknowledgments

I want to sincerely thank my guide, Dr. S. Krishna Prasad, for their invaluable guidance and support throughout my Visiting Student Program. Their expertise and encouragement helped me to complete this research and write this report. He provided me with the necessary data sets used in this project and also helped me gain the necessary insights in the field of Solar Physics.

I would also like to thank the Aryabhatta Research Institute of Observational Sciences for this opportunity and for letting me work in their aesthetic campus.

I also thank my friend Sarwin Chandran for helping me with the coding.

Abstract

The Solar Acoustic halo effect is characterized by an acoustic power enhancement at higher frequencies (> 5.5 mHz) than the typical p-mode frequencies. We analyze the data from *Helioseismic Magnetic Images* (HMI) and *Atmospheric Imaging Assembly* (AIA) instruments on board the *Solar Dynamics Observatory* (SDO by NASA) to characterize the spatio-temporal acoustic power distribution in active regions as a function of the height in the Solar Atmosphere. For this, we use Continuum intensity observed using Magnetically sensitive line at 6173 Åand Doppler-gram as well as intensity at 1600 Åand 1700 Å. We study the power enhancement around the Sun Spot **NOAA 12381** of $\boldsymbol{\beta\gamma}$ class and the Solar Pore **NOAA 12378** of $\boldsymbol{\alpha\gamma}$ of as a function of wave frequency, magnetic field strength, field inclination and observation height. We find that acoustic halos occur in the frequency around the range of **8** mHz. Halos are found to be strong functions of Magnetic field strength forming around the field range of **50G -200G**. We further see the formation of structures with higher relative power around the Inter-network regions, with the structure becoming more pronounced only in higher frequencies.

Keywords:

Power Maps, Fourier Analysis, Magnetic fields, Active regions, Field strength, Observations, Photosphere, Chromosphere, Data cubes, Waves, frequencies, Sun Spots, Solar Pore

Contents

List of Figures

Chapter 1

Introduction

Here comes the Sun ...

– The Beatles

Enhanced power of high-frequency waves surrounding strong-magnetic field structures observed in the Solar Atmosphere. This excess power is known as "Acoustic Halo", first observed in early 1990's at photospheric (Brown *et* al., 1992) as well as chromospheric (Braun *et* al., 1992) heights, at frequencies above the photospheric cut-off of $\approx$ 5.3 mHz, in the range of 5.5 - 7 mHz, and over regions of weak to intermediate strength (50 - 250 G) photospheric magnetic field. A good number of observational studies since then, have brought out additional features. On theoretical side, no single model describing all of the observed features has been achieved yet, although there have been several focused efforts (Hanasoge, 2009; Khomenko, E. and Collados, M. (2009). However, a large number of studies centered around modeling acoustic wave - magnetic field interactions over heights from the Photosphere to Chromosphere, with relevance to high frequency power excess observed around Sunspots, have been carried out (Khomenko and Collados (2006); Rosenthal et al. (2002); Khomenko, E. and Collados, M. (2009)).

Some of the characteristics noted by the observations on the Halos can be summarized as follows:

(i) The power enhancement is observed at high frequencies, between 5.5 and 7.5 mHz for waves that are usually non-trapped in the non-magnetic quiet Sun.

(ii) The Acoustic power measured in Halos is higher than in the nearby quiet Sun by about 40-60% (Hindman & Brown 1998; Braun & Lindsey 1999; Donea *et* al. 2000; Jain & Haber 2002; Nagashima *et* al. 2007);

(iii) The halos are observed at intermediate longitudinal Magnetic flux region i.e. $\langle \boldsymbol{B} \rangle$ = 50-300 G, while the acoustic power is usually reduced at all frequencies at larger fluxes (Hindman & Brown 1998; Thomas & Stanchfield 2000; Jain & Haber 2002);

(iv) the radius of the Halo increases with height. In the photosphere the Halos are located at the edges of active regions, while in the chromosphere they extend to a large portion of the nearby quiet Sun (Brown *et* al. 1992; Braun *et* al. 1992; Thomas & Stanchfield 2000);

(v) the power increase in the Halo is qualitatively similar in Sunspots, Pores and Plages;

(vi) Significant reflection of the upcoming acoustic radiation at 5-6 mHz is detected in active regions, unlike the behavior of such high-frequency waves in the quiet Sun (Braun & Lindsey 2000).

1.1 Data and Analysis Method

We use data from *Helioseismic and Magnetic Imager* (HMI) and *Atmosphere Imaging Assembly* (AIA) onboard the *Solar Dynamics Observatory* (SDO): Photospheric Doppler Velocity [$\boldsymbol{v}$], Continuum intensity [$\boldsymbol{I_c}$], Vector Magnetic field [$\boldsymbol{B_x}$, $\boldsymbol{B_y}$, and $\boldsymbol{B_z}$] derived from HMI observations, and Chromospheric UV emissions observed by AIA in the wavelength channels 1700 Å and 1600 Å, which we denote as $\boldsymbol{I_{uv1}}$ and $\boldsymbol{I_{uv2}}$, respectively. The intensities $\boldsymbol{I_{uv1}}$ and $\boldsymbol{I_{uv2}}$ are now known to capture clear oscillation signals due to Helioseismic p-modes as well as propagating waves in the atmosphere (Howe et al. (2012); Hill *et al., 2011*). The Photospheric observations by HMI are in the form of filtergram images captured from across the Magnetically sensitive line Fe I 6173.34 Å. The AIA imager has the cadence of 24 sec and HMI imager has the cadence of 45 secs. Here the analysis is done on 2 active regions namely: **NOAA 12381** with 2 Sunspots of $\boldsymbol{\beta\gamma}$ class and **NOAA 12378** with 2 Solar Pores of $\boldsymbol{\alpha\gamma}$ class. Our chosen active regions **NOAA 12381** and **NOAA 12378**, have a spatial size of $\boldsymbol{218Mm \times 218Mm}$ and $\boldsymbol{218Mm \times 363Mm}$ with a spatial resolution of **0.6**arcsecond per pixel. The images comprises of one hour long data on the date: $\boldsymbol{2015-07-10, 07:00:40}to\boldsymbol{07:59:55}$. Both AIA and HMI data are co-aligned in IDL programming language through tracking and remapping. The vector Magnteic field has the data on Field strength, Field inclination and Azimuth components of the field.

It should be noted that we have the data from 4 different heights above the Continuum optical depth $\boldsymbol{\tau = 1}$ (z = 0 km) level (Norton *et* al., 2006): $\boldsymbol{I_c}$ is from about $\boldsymbol{z = 0}$ km, $\boldsymbol{v}$ corresponds to an average height of about $\boldsymbol{z = 140}$ km (Fleck, Couvidat and Straus, 2011). The AIA 1700 Å and 1600 Å intensities [$\boldsymbol{I_{uv1}}$

and $\boldsymbol{I_{uv2}}$], form at average heights of 360 km and 430 km (Fossum and Carlsson (2005)), respectively. Thus, we have velocities and intensities from at least four different heights ranging from $\boldsymbol{z = 0}$ to **430** km. Figure 1.1 represents the data in the four layers from $\boldsymbol{z = 0km}$.

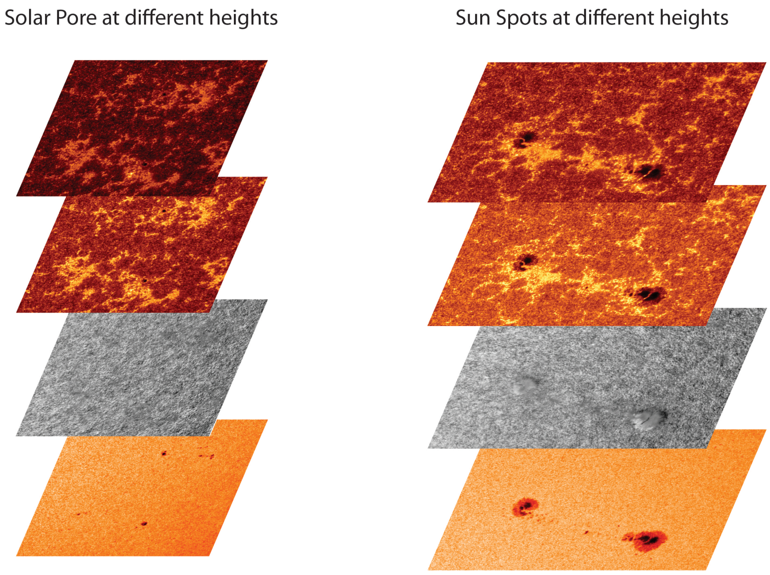

Figure 1.1: a) Solar Pore b) Sun Spots at different heights
Continuum, Doppler-gram, AIA 1700 Åand AIA 1600 Å

Table 1.1: Instrument and Observation Details

Instrument/ Observable	**Spatial Sampling (arcs/pixel)**	**Cadence (sec)**	**Line Formation Height (km)**	**Start Time**	**End Time**
HMI/Doppler	0.6	45	140	2015.07.10 07:01:38	2015.07.10 08:00:53
HMI/Continuum	0.6	45	0	2015.07.10 07:01:38	2015.07.10 08:00:53
AIA 1700 Å	0.6	24	360	2015.07.10 07:00:16	2015.07.10 07:59:52
AIA 1600 Å	0.6	24	430	2015.07.10 07:00:16	2015.07.10 07:59:52

1.2 Making Power maps

Power maps are an important diagnostic tool that is extensively used in Helioseismology to map the distribution of Power in different frequency band. We are using

Fourier transform over Wavelet transform for it high resolution in frequency domain and we are not in need of time information that is provided by the Wavelet analysis, but one can use it for the analysis as the oscillations in the Sun is intermittent and if information about the time is of some interest in the analysis.

Power Maps gives us a way to deduce the power coming off a patch of the image at a particular frequency band. Fourier transform method is employed to deduce the power at different frequency band. We do this transform at every pixel of the chosen active region and construct an image by choosing a particular frequency band. It has to be noted that since the data is in a discrete form, we are limited by the maximum frequency that we probe in these Power maps. The limiting frequency is defined by Nyquist frequency which is the highest frequency that equipment of a given sample rate can reliably measure, one-half the given sample rate. Therefore, the maximum frequency that can be probed for the HMI's 45 sec and AIA's 24 sec cadence data is 11.1 mHz and 20.8 mHz respectively. But in our analysis we are only considering to the maximum of 11 mHz, hence are not affected by the limiting condition, posed by the discrete data-set.

The formula for Discrete Fourier transform is given by

$$\boldsymbol{\hat{x}_n = \sum_{k=0}^{N-1} x_t e^{2\pi\iota k_n/N} \qquad\qquad k_n = \pm 0, \pm 1, \ldots, \pm(N/2-1)}$$

Here $\boldsymbol{\hat{x}_n}$ is the amplitude in the discrete frequency domain, $\boldsymbol{x_t}$ is the amplitude in the time domain and $\boldsymbol{N}$ being the length of the data-set containing images. The frequency that we choose to make Power Maps are as follows: *High frequency* = 7-11 mHz and *Low frequency* = 3-5 mHz. The reason to choose the low frequency is that it contains the frequency higher than the Photosphereic cut-off for a region with Magnetic field and is also shown by S.P. Rajaguru (2012), that these frequencies are significantly suppressed in the Power Maps.

We then go ahead and make scatter plots to study the dependence of the Power release with the Field strength and the inclination. This gives a tool to pinpoint the region where the Power enhancement can be expected to be visible, and to note if the Magnetic Halos have co-relation with the Field strength and Inclination.

Chapter 2

Results

In this chapter we will look into the results that we get with our analysis of the given data. We construct and analyse the Power maps in different frequency band and notice the Spatial reorganisation of Power around the active regions with significant Magnetic field Strength. Figure 2.1 portrays the regions of consideration in the scatter plot.

Power maps were made and layered in *z-axis* with increasing height with Continuum power map being the lowest and AIA 1600 Å being in the top. The values of Power are normalised with respect to the Quiet-Sun power.

For the *Power vs Magnetic field strength* plot we consider the region traced by the rectangle in the images, which has the Active regions and some part of Quiet Sun. Whereas for the *Power vs Inclination* plot we tried removing the regions with vertical magnetic field to isolate the inclined field region. The power that we are consider here is Normalised with respect to Quiet-Sun power (as done by S. C. Tripathy (2017)).

The main focus of this study is to analyse the Power Halos around the Solar Pore region the study of which has not been done yet. The Power maps show consistent signatures of Power Halo in the regions with intermediate Magnetic field in the high frequency maps. Whereas the low frequency maps show a significant suppression of Power around the same active regions. A slight increase in the Halo size can is also evident among the Power Maps of AIA 1600 Å and 1700 Å. One can also notice that there is no such structure visible in the Continuum Power map, which is suggested by Hindman & Brown 1998; Jain & Haber 2002. The Dopplergram image do not show a Power Halo but does show a suppression of the energy in both low and High frequency band. I think it is the "*Magnetic shadow*" predicted by Nutto, C. et al. (2012), where they did a 3-D radiation MHD simulations of the surface layers of the Sun and found a region of lower energy around the Network regions. They made a Power map of the vertical velocity perturbation, $\boldsymbol{\delta v_z}$, in the lower chromosphere. Although I can't be sure with this as the Dopplergram might contain the rotation effect which can't be easily isolated as the Active regions we chose are 23° (Sunspots) and 19° (Solar pores) away from the disk centre. This effect has not been removed yet and reminiscent of which can be seen across the Dopplergram Power map, with it being bright on one side and dark on the other

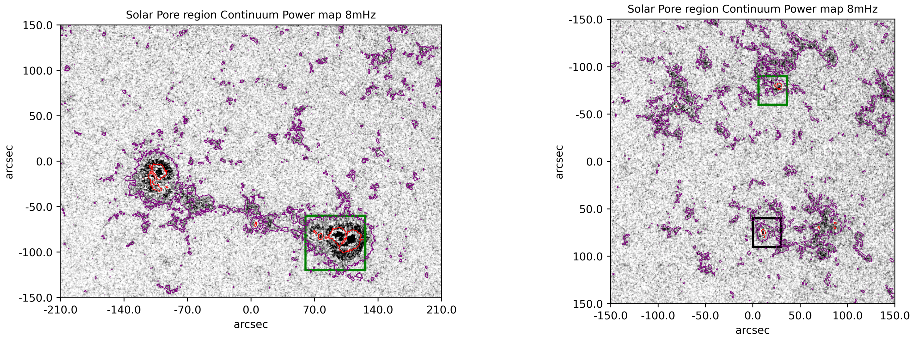

Figure 2.1: Contours over the Power Maps of the continuum
The purple contours denote the regions with the Field strength of 200 G and the inner red contour denotes the region with the field strength of 1500 G a) The Sunspots b) The Solar Pore

2.1 Power Maps

The Power maps are then made for high and low frequency range. The color-map chosen for the plot is known as "*Viridis*", chosen its *Perceptually Uniform Sequential* property. In the Figure 1.1 one can notice a "*Light bridge*" in the lower Sunspot, dividing the Sunspot into two. This shows itself in the Power maps in Figure 2.2 as a bright line withing the lower Sunspot.

It can be noted that the regions where the Power Halos are note closely matches with the "*Plages*" in the Solar surface. The reason being that these plages have intermediate field strength with significant inclination of the field to satisfy the conditions for Halos to occur.

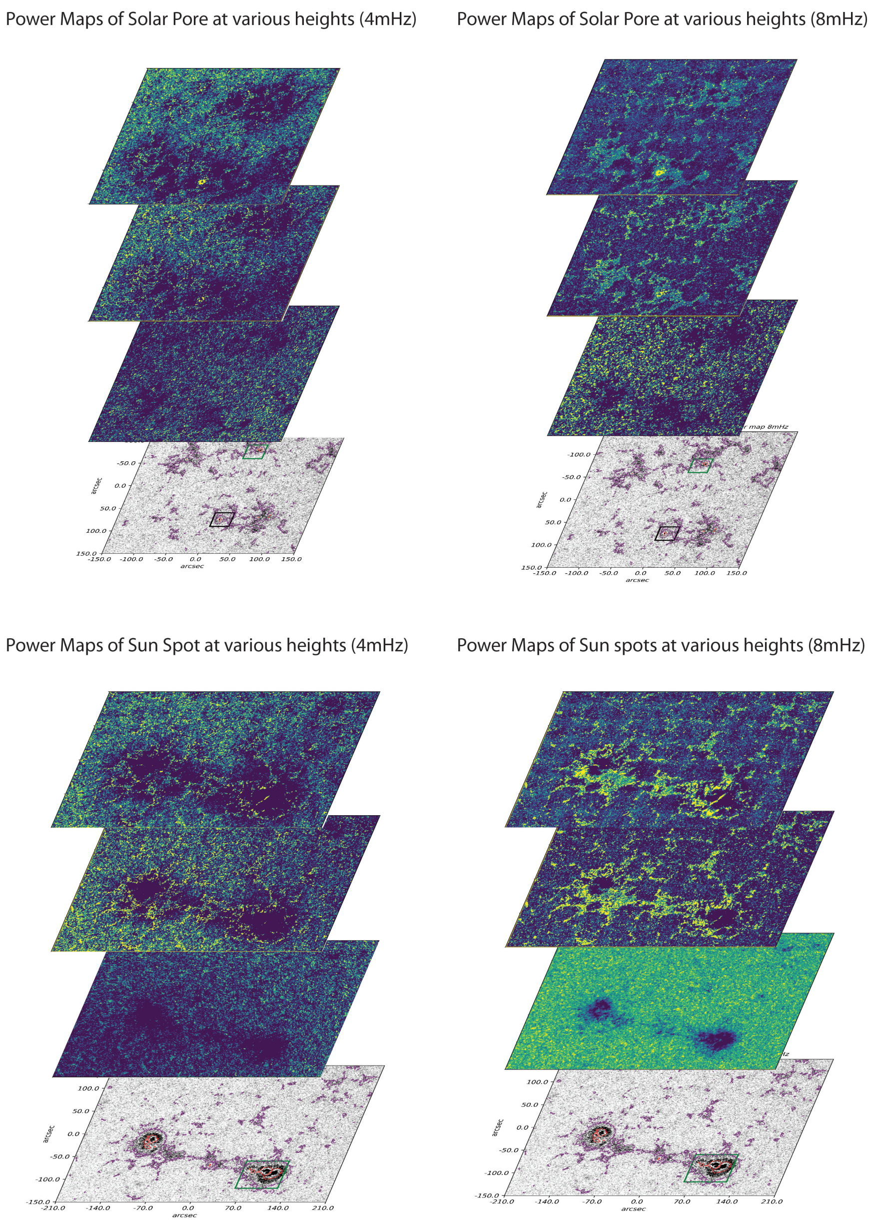

Figure 2.2: The Spatial reorganisation of the high frequency Power is clearly visible in Figures b) and d) and in Figure a) and c) a significant Suppression of low frequency power is also seen in the regions surrounding high magnetic field (i.e. around the Active regions)

2.2 Dependence on Field strength and Inclination

In this section we will study the dependency of the Halo structure with the field strength and inclination. Figure 2.3 is for the Sunspots that are present in the data. The line plot is the values averaged over a particular field bin (kind of similar to a running average but for a scatter plot).

We now focus on the AIA 1600 Å and 1700 Å scatter plots of field strength, in Figure 2.3. The plots of 4 mHz show a monotonous decrease in the Power as the field strength increases. There seems to be a distinct peak in the AIA 1600 Å of 1st Sunspot in low frequency, this corresponds to the light bridge that we observe in the continuum image, however the overall behaviour when looked at other low frequency plot, shows a decrease in the Power. As opposed to this, the high frequency plots show a distinct peak in the values close to 200 G. This is where we expect the Halo formation to occur. This value is in agreement with the range suggested by Khomenko, E. and Collados, M. (2009); S.P. Rajaguru (2012). We notice that in the Continuum plot the values are uniform and decreases significantly only at higher magnetic field, suggest no Halo formation, which is also shown by Hindman & Brown 1998; Jain & Haber 2002. The Dopplergram plots do not show the profile similar to AIA data, which I think is due to the limb effects mentioned earlier. But, when we look at the inclination plot, the line doesn't have a profile that provides some conclusion. This is due to the improper threshold value applied while data analysis, there are too many things like errors in Vector Magneto-gram, unwanted pixels in the *Penumbral* region and lack of distinction between wanted and unwanted region in the region. This can be done in the further analysis part in the future.

We then look at the scatter plots of Solar Pore, Figure 2.4. Here too one can see a suppression in the low frequency range, at least in the 2nd Solar Pore. The first Pore had a transient event going on close by which might have caused the peaks that are visible in the first AIA 1600 Å plot. However the rest of the AIA plots are showing a significant decrease in the power with increasing field strength. As opposed to this the scatter plots of the 8mHz shows a distinct peak near the 200 G region, confirming the presence of Halo structure around it. As seen in Figure 2.3, the Continuum power shows a uniform profile only decreasing for the high field strength. When we look at the inclination plot, there is a visible peak at higher inclination angles, which is a necessary condition for the Halo formation, also suggesting the presence of an enhanced power region around the Pore. Doppplergram plot is again contaminated by the rotation effects showing no conclusive evidence for the Halos.

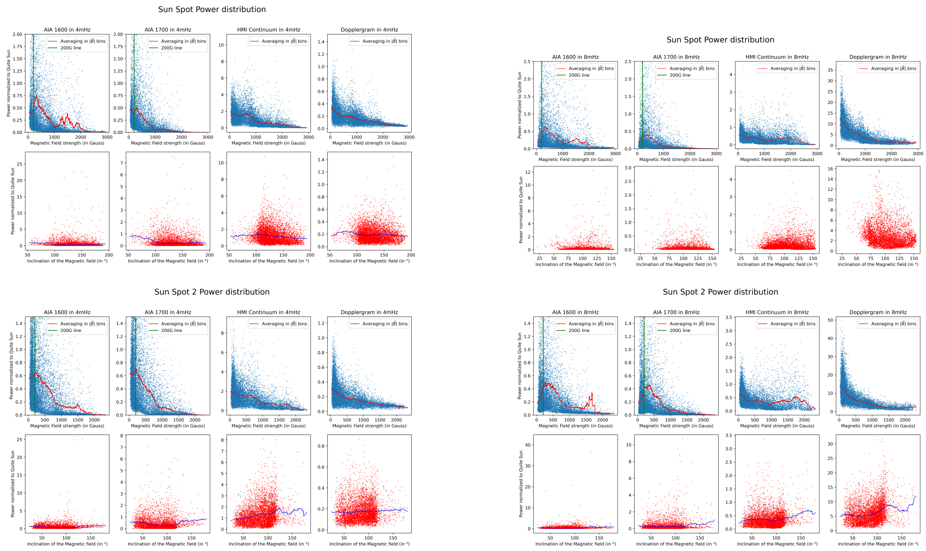

Figure 2.3: Scatter plots for Sun Spots a) and c) figure's AIA 1600 Å and 1700 Å scatter plots shows a more or less monotonous decrease in the Power as the magnetic field increases, where as b) and d) shows a distinct peak near the 200 G line which lies in the range where we are supposed to see a Halo. The red plots are the plots of *Power vs Inclination*, which doesn't exactly show a peak for the reason discussed in Chapter 2.3

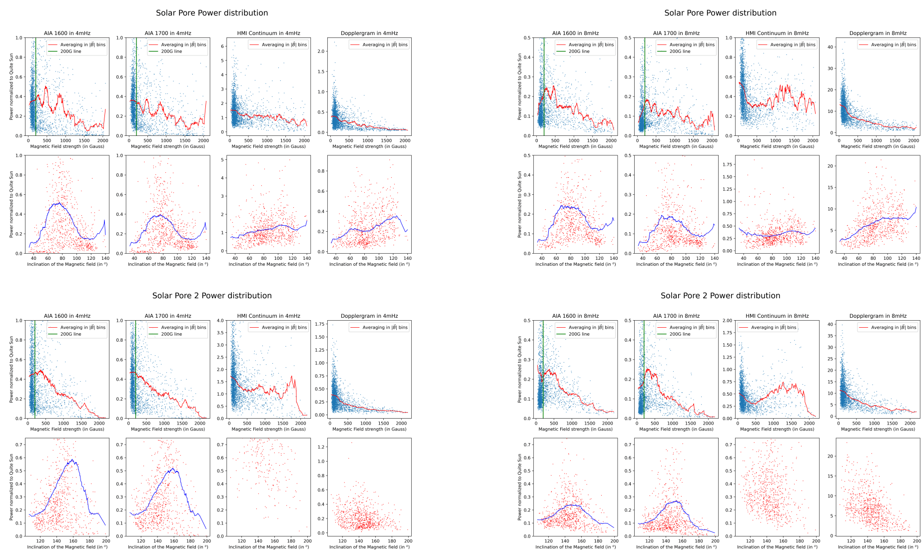

Figure 2.4: Scatter plots for Solar Pores same as Figure 2.3 a) and c) do not show any distinct peak near the 200 G region whereas b) and d) show a peak. Here the red scatter plots show a peak in the centre where the inclination is high.

2.3 Conclusions and discussion

In the analysis, the results are in agreement with the previous literature that has been made around the Halos. The results suggest that there is a formation of

Halos around the active regions with intermediate field strength, and also the enhancement of power in the region with significant inclination. I refer to the simulations conducted by Khomenko, E. and Collados, M. (2009), where they have done multiple simulations on *Monochramatic* and *Gaussian* profile acoustic wave source and show that indeed that the radius of the halo increases with height, showing agreement with their suggested model. I also state that our analysis confirms the observation done by S.P. Rajaguru (2012); where they see a significant amount of enhancement of Power in the 100 - 200 G and 200 - 450 G region.

We conclude that in our analysis we have found evidence that supports *Mode conversion* to be the possible mechanism behind the formation of Halos in the upper Atmosphere of the Sun.

2.4 Further Analysis

i The dependency of the Halo with the inclination, shows some discrepancy with the predictions due to the dilution of the data by the *Penumbral* Magnetic field as discussed in the earlier section. The data needs to be filtered more with necessary methods so that we can make an informed conclusion out of the Sunspot data.

ii Choosing a better Active region that is close by to the disk center at the time of observation might also diminish the effects posed in the Dopplergrams due to this.

iii An $\boldsymbol{\alpha}$ class Sunspot would be great to study the Halos due to its symmetric profile and the absence of plages around it.

iv Further refining of the scatter plots needs to be done by setting appropriate threshold in choosing the region of analysis.

v Ground based data would fetch us greater resolution by which one can probe to the regions around the Pores which needs high resolution due to its small size. This can help us make more definite conclusions on the Halos.

References

Fossum, A. and Carlsson, M. (2005). High-frequency acoustic waves are not sufficient to heat the solar chromosphere. *Nature*, 435(7044):919–921.

Howe, R., Jain, K., Bogart, R. S., Haber, D. A., and Baldner, C. S. (2012). Two-dimensional helioseismic power, phase, and coherence spectra of solar dynamics observatory photospheric and chromospheric observables. *Solar Physics*, 281:533–549.

Khomenko, E. and Collados, M. (2006). Numerical modeling of magnetohydrodynamic wave propagation and refraction in sunspots. *The Astrophysical Journal*, 653(1):739.

Khomenko, E. and Collados, M. (2009). Sunspot seismic halos generated by fast mhd wave refraction. *A&A*, 506(2):L5–L8.

Nutto, C., Steiner, O., and Roth, M. (2012). Revealing the nature of magnetic shadows with numerical 3d-mhd simulations. *A&A*, 542:L30.

Rosenthal, C., Bogdan, T., Carlsson, M., Dorch, S., Hansteen, V., McIntosh, S., McMurry, A., Nordlund, Å., and Stein, R. (2002). Waves in the magnetized solar atmosphere. i. basic processes and internetwork oscillations. *The Astrophysical Journal*, 564(1):508.

S. C. Tripathy, K. Jain, S. K. F. H. S. P. R. P. S. C. (2017). A study of acoustic halos in active region noaa 11330 using multi-height sdo observations. *Advances in Space Research*.

S.P. Rajaguru, S. Couvidat, X. S. K. H. H. S. (2012). Properties of high-frequency wave power halos around active regions: An analysis of multi-height data from hmi and aia onboard sdo. *Springer, Solar Physics*.